

Myosin dynamics in live *Dictyostelium* cells

(green fluorescent protein)

SHERI L. MOORES, JAMES H. SABRY, AND JAMES A. SPUDICH

Departments of Biochemistry and Developmental Biology, Stanford University School of Medicine, Stanford, CA 94305

Contributed by James A. Spudich, October 3, 1995

ABSTRACT Conventional myosin plays a key role in the cytoskeletal reorganization necessary for cytokinesis, migration, and morphological changes associated with development in nonmuscle cells. We have made a fusion between the green fluorescent protein (GFP) and the *Dictyostelium discoideum* myosin heavy chain (GFP-myosin). The unique *Dictyostelium* system allows us to test the GFP-tagged myosin for activity both *in vivo* and *in vitro*. Expression of GFP-myosin rescues all myosin null cell defects. Additionally, GFP-myosin purified from these cells exhibits the same ATPase activities and *in vitro* motility as wild-type myosin. GFP-myosin is concentrated in the cleavage furrow during cytokinesis and in the posterior cortex of migrating cells. Surprisingly, GFP-myosin concentration increases transiently in the tips of retracting pseudopods. Contrary to previous thinking, this suggests that conventional myosin may play an important role in the dynamics of pseudopods as well as filopodia, lamellipodia, and other cellular protrusions.

Although the function of conventional myosin in muscle cells has been well established for many decades, the roles this actin-based motor plays in nonmuscle cells have been addressed only more recently. Unlike skeletal myosin in a sarcomere, nonmuscle myosin is not confined to a fixed structure and so is able to assemble and disassemble as needed in the cell. These changes in myosin distribution contribute to the continual reorganization of the cell's structure that is required for normal cellular function. Myosin has been shown to be involved in cytokinesis, migration, capping of surface receptors, and development in the eukaryote *Dictyostelium discoideum* (1, 2). With use of immunofluorescence labeling techniques on fixed cells, myosin has been seen in the cleavage furrow of dividing cells, in the posterior cortex of migrating cells, and under caps of surface receptors in cells stimulated with concanavalin A (3, 4). Although these localizations are informative, they remain single images during dynamic processes and as such, provide only partial descriptions. In the present work we have tagged myosin with the green fluorescent protein (GFP) and expressed this GFP-myosin fusion protein in myosin null cells to follow myosin movements in live *Dictyostelium* cells.

MATERIALS AND METHODS

Plasmid Construction. A GFP-myosin expression plasmid was constructed as follows. A 2.1-kb fragment containing the *Dictyostelium* actin-15 gene promoter fused to the 5' end of the *Dictyostelium mhca* gene (5) was modified to create a *Bam*HI site at the start codon of the *mhca* gene (K. Ruppel and J.A.S., unpublished data) and inserted into pBluescript II KS to create pBS-MyBam. An in-frame fusion of the GFP coding sequence to the 5' end of the *mhca* gene was achieved as follows. The plasmid pGFP10.1 contains the GFP cDNA (6) and was used

as a template for PCR. Primers were designed to maintain the same reading frame with *mhca*, while adding a *Bam*HI site to the 5' end and a *Bgl* II site to the 3' end of GFP sequence. Additionally, the 5'-end primer changed GFP codons 2 and 4 to match more closely *Dictyostelium* codon preference. The sequence of the 5'-end primer was 5'-CGCGGATCCATCAAAGGTGAAGAACTTTTCACTG-3', and the sequence of the 3'-end primer was 5'-GAAGATCTTTGTATAGTTCATCCATGCC-3'. The PCR product was digested with *Bam*HI and *Bgl* II and inserted into *Bam*HI-digested pBS-MyBam to create pBS-GFPmyo. The appropriate *Xba* I-*Bst*XI fragment from pBS-GFPmyo was inserted into *Xba* I-*Bst*XI-digested pBigMyD, which contains the full-length wild-type *mhca* gene in an extrachromosomal *Dictyostelium* expression plasmid (5), to create pBigGFPmyo.

Growth of *Dictyostelium* Cells. *Dictyostelium* cells were grown in HL-5 medium (7) supplemented with 60 units of penicillin and 60 μ g of streptomycin per ml at 21°C. Transformations were performed using electroporation as described (8). Transformed cells were selected and grown in the presence of G418 at 5 μ g/ml (Geneticin; Life Technologies, Gaithersburg, MD). The myosin null cell line HS1 (5) was transformed with either pBigMyD to create wild-type myosin cells (5) or pBigGFPmyo to create GFP-myosin cells. To observe development, cells were spotted onto *Klebsiella aerogenes* lawns on SM agar plates (7).

Electrophoresis. Duplicate lanes of whole-cell lysates were electrophoresed on a single SDS/7.5% polyacrylamide gel. Half was stained with Coomassie brilliant blue, and the other half was transferred to nitrocellulose. The filter was probed with My6, an anti-*Dictyostelium* myosin antibody (9) followed by a horseradish peroxidase-coupled secondary antibody (Bio-Rad). Signals were visualized with an enhanced chemiluminescence system (DuPont).

Protein Purification. GFP-myosin was purified from *Dictyostelium* cells as described for wild-type myosin (5). The purified GFP-myosin protein was treated with bacterially expressed myosin light-chain kinase, and the phosphorylation level of the regulatory light chain was assayed by urea/SDS/glycerol/polyacrylamide gel electrophoresis as described (5). The concentration of the purified GFP-myosin was determined by the Bradford method (10) with rabbit skeletal muscle myosin as the standard.

Imaging. *Dictyostelium* amebae expressing GFP-myosin were plated on 25-mm glass coverslips and bathed in Mes buffer (20 mM MES, pH 6.8/0.2 mM CaCl₂/2 mM MgSO₄) at 22°C. The cells were visualized with a Zeiss Axiovert microscope using a Planapochromat 100/1.4 objective and a base-ment port connected to a cooled charge-coupled device (CCD) camera (Photometrics, Tucson). The camera was connected to the microscope with standard relay optics configured so that each camera pixel received light from a 100 nm \times 100 nm square element of the specimen. This allows the resolution to be set by the wavelength of light rather than by the camera itself. For GFP this resolution is approximately 300 nm (11).

The publication costs of this article were defrayed in part by page charge payment. This article must therefore be hereby marked "advertisement" in accordance with 18 U.S.C. §1734 solely to indicate this fact.

Abbreviation: GFP, green fluorescent protein.

Images were taken every 5 sec with the light shuttered to allow a 20-msec exposure from a 100-W Hg lamp attenuated with a 50% neutral density filter. This was required to prevent light-induced damage to the cells. The light was filtered with a HiQ fluorescein or GFP filter set (Chroma Optics, Brattleboro, VT). Images were collected and analyzed with Image-1/Metamorph (Universal Imaging, West Chester, PA). The cell shown in Fig. 2*b* was fixed in cold methanol (-10°C) for 10 min and then imaged on a confocal microscope (Molecular Dynamics).

RESULTS AND DISCUSSION

To follow the movements of myosin in live cells, a fusion between the GFP and myosin was created. Plasmids were constructed to express either the wild-type *Dictyostelium* myosin heavy chain or the GFP protein linked to the N terminus of *Dictyostelium* myosin heavy chain, transformed into a myosin null cell line, and independent clones were isolated. The GFP-myosin fusion protein was expressed *in vivo* at the same level as wild-type myosin but migrated more slowly than the 210-kDa wild-type myosin heavy chain in SDS electrophoretic gels, consistent with the addition of 238 amino acids from GFP (12) (Fig. 1).

Expression of GFP-myosin fully complemented the myosin null cell phenotype. Myosin null cells cannot undergo cytokinesis and therefore fail to grow in suspension culture (13, 14). In contrast, cells expressing either wild-type myosin or GFP-myosin grew normally in suspension (data not shown). Myosin null cells fail to complete the *Dictyostelium* developmental cycle, arresting at the "mound stage" (13, 14). Expression of either wild-type myosin or GFP-myosin allowed the cells to complete the full developmental cycle, culminating in the construction of fruiting bodies (data not shown).

To compare the *in vitro* activities of GFP-myosin to wild-type myosin, GFP-myosin was purified from *Dictyostelium* cells, treated with bacterially expressed *Dictyostelium* myosin light-chain kinase, and assayed for actin-activated ATPase activity as described (5). In low-salt Mg^{2+} buffer, GFP-myosin had a low basal activity of 0.03 μmol of phosphate released per min per mg of myosin. Addition of actin increased the ATPase activity to 0.20 $\mu\text{mol}/\text{min}$ per mg. These values agree well with the ranges of values observed for wild-type myosin: 0.015–0.030 $\mu\text{mol}/\text{min}$ per mg for basal activity and 0.15–0.19 $\mu\text{mol}/\text{min}$ per mg for actin-activated activity (ref. 5; K. Ruppel and J.A.S., unpublished data). Next, the ability of purified GFP-myosin to move actin filaments was measured at 30°C using an *in vitro* motility assay (15). GFP-myosin moved actin

filaments at a rate of 2.2 $\mu\text{m}/\text{sec}$. This value is within the range of velocities measured for wild-type myosin: 1.9–3.1 $\mu\text{m}/\text{sec}$ (5, 16, 17).

When *Dictyostelium* amebae expressing GFP-myosin were imaged, the fluorescence was concentrated in the cell cortex but also was distributed diffusely throughout the cytoplasm (Fig. 2*a*). GFP-myosin was concentrated in the cleavage furrow during cytokinesis and in the posterior region of migrating cells (Fig. 2*a* and *b*). This distribution is similar to that seen by immunofluorescence in fixed cells (4, 18, 19). An unexpected finding that could only have been seen by time-lapse imaging of live cells was a transient focal concentration of GFP-myosin in the tips of retracting pseudopods (Fig. 2*c–e* and *f–h*). This brief local increase in concentration occurred concurrent with the early stages of pseudopod retraction and often terminated well before the retraction was complete (Fig. 2*c–e* and *f–h*). The concentration changes of GFP-myosin in retracting pseudopods occurred over seconds suggesting that myosin is rapidly rearranged in the cell. Changes in GFP-myosin concentration never occurred in pseudopods during their protrusion. The concentration of the fluorescence in retracting pseudopods, the posterior end of migrating cells, the cellular cortex, and the cleavage furrow was not seen when GFP alone was expressed (data not shown).

X-ray crystallographic studies of myosin suggest that GFP fused to the N terminus of myosin might be expected to sit upon the central globular region of the myosin catalytic domain (20, 21). This location would place the GFP away from the actin-binding face and nucleotide-binding regions of the molecule, permitting normal myosin function. In a recent study, binding of an antibody raised against a peptide consisting of myosin residues 1–7 to the S1 fragment of rabbit skeletal muscle myosin had no effect on ATPase activities nor binding of S1 to actin (E. Reisler, personal communication). This supports the idea that relatively large molecules can be attached to the N terminus of myosin without affecting its activity.

Because expression of the GFP-myosin fusion protein restored wild-type behavior to myosin null cells and because purified GFP-myosin protein displayed wild-type myosin properties *in vitro*, it is likely that the location of this protein in live *Dictyostelium* cells is an accurate representation of the location of wild-type myosin *in vivo*. Observing myosin movements in live cells over time offers several advantages over observing samples of fixed cells. First, artifacts associated with fixation procedures are avoided. Second, accurate dynamic measurements can be made *in vivo* and correlated with *in vitro* measurements of protein function. For example, certain myosin mutations affect the speed with which myosin moves *in vitro* (ref. 16; T. Uyeda, P. Abramson, and J.A.S., unpublished data). Therefore, it is reasonable to expect that the velocity with which these mutated myosins perform their *in vivo* functions, such as cytokinesis, may be similarly altered. Measurements of these myosin-based events *in vivo* can now be made with high temporal resolution. Finally, dynamic events can be followed in their natural temporal context. This is best illustrated by our observation of the transient concentration of GFP-myosin in retracting pseudopods.

The mechanical basis of pseudopod dynamics is not well understood, but the forces involved have been attributed to actin assembly or certain actin-based motors (22). The best candidates for such motors to date have been the unconventional myosins (myosin I type), which are found in pseudopods in *Dictyostelium* and neuronal growth cones (4, 23). The concentration of conventional myosin in the tips of pseudopods only when they are retracting suggests that different motors may be involved in different phases of pseudopod dynamics, with conventional myosin playing a role only in retraction. Furthermore, this novel localization suggests that conventional myosin may play a role in the retraction of other cellular protrusions such as neuronal growth cone filopodia

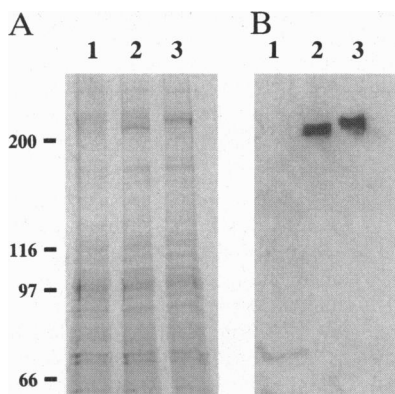


FIG. 1. Expression of GFP-myosin in *Dictyostelium* cells. (A) Coomassie-stained gel. (B) Immunoblot. Lanes: 1, myosin null cells; 2, wild-type myosin cells; 3, GFP-myosin cells. No myosin was expressed in myosin null cells. GFP-myosin and wild-type myosin were expressed at the same level, but GFP-myosin migrated more slowly than wild-type myosin. Sizes are in kDa.

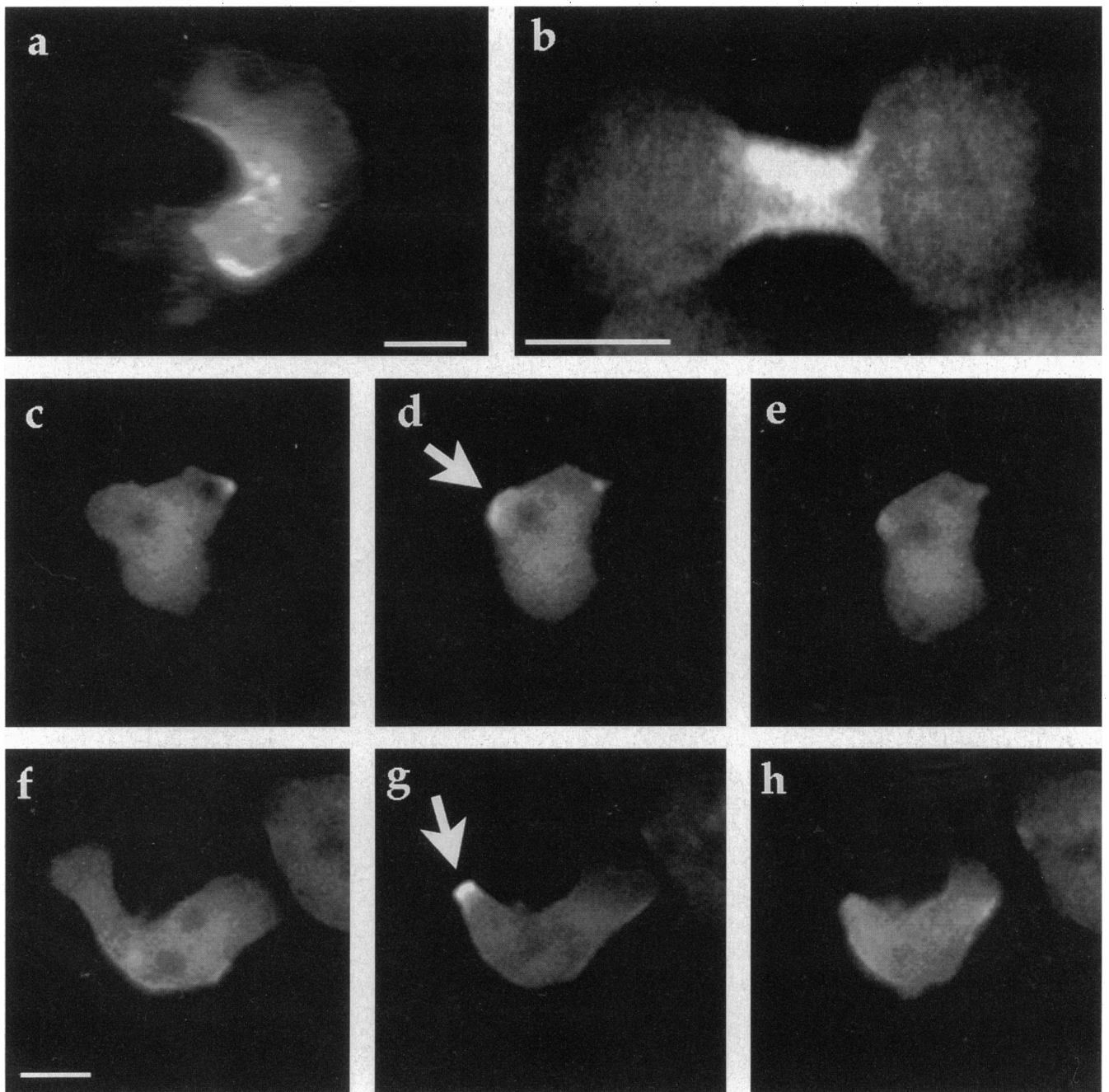


FIG. 2. Localization of GFP-myosin in *Dictyostelium* cells. (a) The cell is migrating to the upper right, and GFP-myosin can be seen concentrated in the posterior or trailing region of the cell. (b) GFP-myosin was also concentrated in the cleavage furrow in a dividing cell. (c–e and f–h) GFP-myosin concentration briefly increased in the tips of retracting pseudopods as shown in two different examples. (d and g) GFP-myosin was concentrated in the pseudopod tip (arrows) in the early stages of retraction. This transient increase in concentration was lost before retraction was complete (e and h). Images in c–e are shown at 10-sec intervals, whereas images in g occurred 35 sec after those in f, and images in h occurred 15 sec after those in g. (Bars = 5 μ m; the bar in f applies to c–h.)

and lamellipodia as well as those in leukocytes and fibroblasts. Interestingly, it has been shown recently that *Dictyostelium* cells lacking conventional myosin have severe defects in retracting cellular attachments from adhesive substrates (24). This supports the hypothesis that conventional myosin is generally required for many diverse contraction events in the cell, including the retraction of cellular attachments.

We thank M. Kirschner for use of his low-light-level imaging facility, G. Manning for assistance with confocal microscopy, K. Ruppel for biochemical guidance, and E. Reisler for sharing unpublished data. In addition, we thank S. Munroe, S. Pfeffer, K. Ruppel, J. Smith, and H. Warrick for critical comments on the manuscript. This work was

supported by grants from the National Institutes of Health to J.A.S.; S.L.M. is supported by a National Institutes of Health training grant, and J.H.S. is supported by the Cancer Research Fund of the Damon Runyon–Walter Winchell Foundation (DRG-073).

1. Warrick, H. M. & Spudich, J. A. (1987) *Annu. Rev. Cell Biol.* **3**, 379–421.
2. Korn, E. D. & Hammer, J. A. (1988) *Annu. Rev. Biophys. Biophys. Chem.* **17**, 23–45.
3. Pasternak, C., Spudich, J. A. & Elson, E. L. (1989) *Nature (London)* **341**, 549–551.
4. Fukui, Y., Lynch, T. J., Brzeska, H. & Korn, E. D. (1989) *Nature (London)* **341**, 328–331.
5. Ruppel, K. M., Uyeda, T. Q. P. & Spudich, J. A. (1994) *J. Biol. Chem.* **269**, 18773–18780.

6. Chalfie, M., Tu, Y., Euskirchen, G., Ward, W. W. & Prasher, D. C. (1994) *Science* **263**, 802–805.
7. Sussman, M. (1987) *Methods Cell Biol.* **28**, 9–29.
8. Egelhoff, T. T., Titus, M. A., Manstein, D. J., Ruppel, K. M. & Spudich, J. A. (1991) *Methods Enzymol.* **196**, 319–334.
9. Peltz, G., Spudich, J. A. & Parham, P. (1985) *J. Cell Biol.* **100**, 1016–1023.
10. Bradford, M. M. (1976) *Anal. Biochem.* **72**, 248–254.
11. Inoue, S. (1986) *Video Microscopy* (Plenum, New York).
12. Prasher, D. C., Eckenrode, V. K., Ward, W. W., Prendergast, F. G. & Cormier, M. J. (1992) *Gene* **111**, 229–233.
13. Knecht, D. A. & Loomis, W. F. (1987) *Science* **236**, 1081–1086.
14. De Lozanne, A. & Spudich, J. A. (1987) *Science* **236**, 1086–1091.
15. Uyeda, T. Q. P., Kron, S. J. & Spudich, J. A. (1990) *J. Mol. Biol.* **214**, 699–710.
16. Uyeda, T. Q. P. & Spudich, J. A. (1993) *Science* **262**, 1867–1870.
17. Uyeda, T. Q. P., Ruppel, K. M. & Spudich, J. A. (1994) *Nature (London)* **368**, 567–569.
18. Yumura, S., Mori, H. & Fukui, Y. (1984) *J. Cell Biol.* **99**, 894–899.
19. Yumura, S. & Fukui, Y. (1985) *Nature (London)* **314**, 194–196.
20. Fisher, A. J., Smith, C. A., Thoden, J., Smith, R., Sutoh, K., Holden, H. M. & Rayment, I. (1995) *Biophys. J.* **68**, 19s–28s.
21. Rayment, I., Rypniewski, W., Schmidt-Base, K., Smith, R., Tomchick, D., Benning, M., Winkelmann, D., Wesenberg, G. & Holden, H. (1993) *Science* **261**, 50–58.
22. Condeelis, J. (1993) *Annu. Rev. Cell Biol.* **9**, 411–444.
23. Ruppert, C., Kroschewski, R. & Bahler, M. (1993) *J. Cell Biol.* **120**, 1393–1403.
24. Jay, P. Y., Pham, P. A., Wong, S. A. & Elson, E. L. (1995) *J. Cell Sci.* **108**, 387–393.